Hydrology Research

Hydrology Research Vol 53 No 1, 193 doi: 10.2166/nh.2021.006

Propagation dynamics and causes of hydrological drought in response to meteorological drought at seasonal timescales

Lan Ma[a], Qiang Huang[a], Shengzhi Huang[a,*], Dengfeng Liu[a], Guoyong Leng[b], Lu Wang[a] and Pei Li[a]

[a] State Key Laboratory of Eco-hydraulics in Northwest Arid Region of China, Xi'an University of Technology, Xi'an 710048, China
[b] Key Laboratory of Water Cycle and Related Land Surface Processes, Institute of Geographic Sciences and Natural Resources Research, Chinese Academy of Sciences, Beijing 100101, China
*Corresponding author. E-mail: huangshengzhi7788@126.com

ABSTRACT

According to the widely accepted definition of drought, meteorological and hydrological droughts originally develop from rainfall and runoff deficits, respectively. Runoff deficit is mainly derived from rainfall deficit, and the propagation from meteorological drought to hydrological drought is critical for agricultural water management. Nevertheless, the characteristics and dynamics of drought propagation in the spatio-temporal scale remain unresolved. To this end, the characteristics and dynamics of drought propagation in different seasons and their linkages with key forcing factors are evaluated. In this study, meteorological and hydrological droughts are characterized by the Standardized Precipitation Index (SPI) and the Standardized Runoff Index (SRI), respectively. Propagation time is identified by the corresponding timescale of the maximum correlation coefficient between the SPI and the SRI. Then, a 20-year sliding window is adopted to explore the propagation dynamic in various seasons. Furthermore, the multiple linear regression model is established to quantitatively explore the influence of meteorological factors, underlying surface features and teleconnection factors on the propagation time variations. The Wei River Basin, a typical Loess Plateau watershed in China, is selected as a case study. Results indicate the following: (1) the propagation time from meteorological to hydrological drought is shorter in summer (2 months) and autumn (3 months), whereas it is longer in spring (8 months) and winter (13 months). Moreover, the propagation rates exhibit a decreasing trend in warm seasons, which, however, show an increasing trend in cold seasons; (2) a significant slowing propagation in autumn is mainly caused by the decreasing soil moisture and precipitation, whereas the non-significant tendency in summer is generally induced by the offset between insignificant increasing precipitation and significant decreasing soil moisture; (3) the replenishment from streamflow to groundwater in advance prompts the faster propagation from meteorological to hydrological drought in spring and winter and (4) teleconnection factors have strong influences on the propagation in autumn, in which Arctic Oscillation, El Niño-Southern Oscillation and Pacific Decadal Oscillation mainly affect participation, arid index and soil moisture, thereby impacting drought propagation.

Key words: drought propagation dynamics, SPI, SRI, teleconnection factors

HIGHLIGHTS

- The propagation dynamics at a seasonal timescale were explored.
- The impacts of diverse factors on the propagation dynamics were investigated. Autumn exhibits a significant increasing propagation time mainly induced by decreasing soil moisture and precipitation.
- Winter shows a significant decreasing propagation time mainly caused by earlier groundwater supply.
- Teleconnection factors exert strong influences on the propagation process in autumn.

GRAPHICAL ABSTRACT

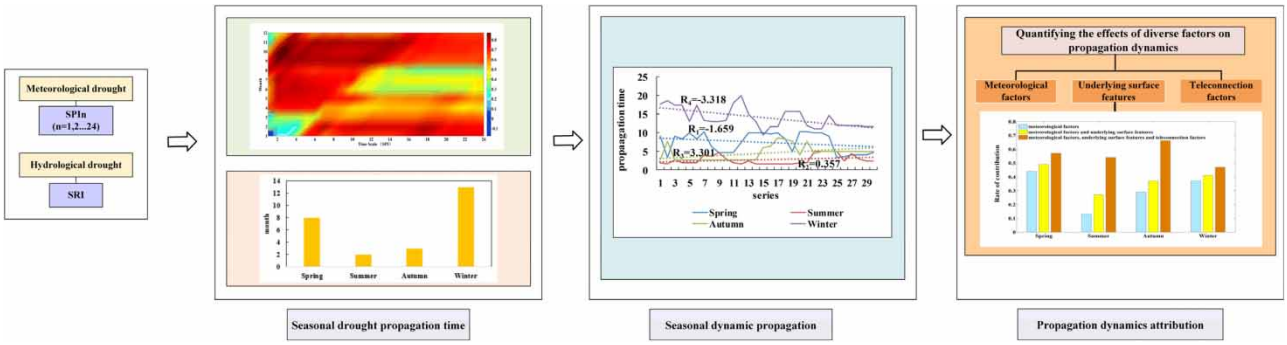

1. INTRODUCTION

With global climate change and intensified water circulation, extreme weather and climate events have become more frequent in recent years. History has repeatedly proved that serious drought events in a given area will not only cause great mortality and economic losses, but also arouse the widespread concern of relevant scholars as well as the introspection of local government. Numerous drought and flood events have occurred in recent decades. A string of drought events occurred in recent decades, thereinto, the sandstorm drought in America of the 1930s (Brekke 1947; Wilhite & Glant 1985; Cook *et al.* 1999; Fye *et al.* 2010), which covered across two-thirds of the United States and wreaking havoc for a decade, caused 250 million people to leave. China has been subjected to drought damage repeatedly in the past years. The year of 2010 in the southwestern of China affected >67,000 km^2 of arable land and left >20 million people without drinking water. The middle and lower reaches of the Yangtze River have suffered the worst drought for a 70-year return period (Yu *et al.* 2014), which impacted 17 million people and the direct economic losses reached nearly 10 billion.

Drought as a natural hazard may happen in all the places (including dry and wet regions) at multiple time scales (Fang *et al.* 2019a, 2019b). It is deemed as a complex, multifaceted phenomenon diffusely (Van Loon 2015), which has a major impact on every part of the hydrological cycle. Moreover, drought can influence wide areas and last for a long time (WMO 1997). Drought has attracted growing attention in many different fields, such as ecology, environment, hydrology and agriculture (Tallaksen & Van Lanen 2004; Mishra & Singh 2010; Zhang *et al.* 2012; Mohammad *et al.* 2014; Chen & Sun 2017). Drought is largely driven by climate changes, such as the decreases of precipitation, which develops slowly and lasts months to years (Tallaksen & Van Lanen 2004; Tallaksen *et al.* 2009). Depending on the deficit of different hydrologic features, drought is commonly divided into four categories, that is, meteorological drought, hydrological drought, agricultural drought and socioeconomic drought (Mishra & Singh 2010). There are some differences and connections between them. Specifically, when the precipitation is insufficient, meteorological drought occurs; the lack of runoff then causes hydrological drought; agricultural drought is triggered by the inadequacy of soil moisture; whereas the socioeconomic drought directly results from the water supply not satisfying the human water demand, which is also the embodiment of the impacts of the above three types of droughts on human society (Dracup *et al.* 1980; Guo *et al.* 2019). In general, meteorological drought begins the earliest, then agricultural and hydrological droughts happen. If the socioeconomic drought occurs finally, this water deficit event is more serious. Many researches have focused on the establishment of drought index, to identify drought events and evaluate spatial and temporal distribution characteristics of drought (Feng *et al.* 2014; Huang *et al.* 2015; Leng *et al.* 2015; Xu *et al.* 2015; Ge *et al.* 2016; Huang *et al.* 2019).

As mentioned above, there are close links between different types of drought. The transformation from one type of drought to another is called drought propagation (Huang *et al.* 2017). In recent years, drought propagation has become a hot topic in the field of hydrology and water resources. The analysis methods of drought propagation are mainly divided into model simulations and statistical methods. Different hydrological models reveal the propagation time between different types of droughts to a certain extent. Wang *et al.* (2011) and Van Loon & Van Lanen (2012) adopted a hydro-agricultural coupling model and an integrated large-scale hydrological model to study the propagation of drought. Lorenzo-Lacruz *et al.* (2013) used the Pearson correlation coefficient to determine the time scale of the Standardized Precipitation Index

(SPI) with the best correlation with the Standardized Runoff Index (SRI) as the response time of hydrological drought to cumulative precipitation deficit. Besides, some researches discuss the forcing factors on drought propagation, for example, the process of propagation from meteorological to hydrological drought is influenced by climate characteristics (Van Loon & Van Lanen 2012). Furthermore, underlying surface features and teleconnection factors also have a great influence on the propagation process (Huang *et al.* 2015, 2017). For the law of drought propagation, Li *et al.* (2018) established the relationship between hydrological drought and driving factors, which can explain this pattern to some extent.

Although multiple researches have inquired into the relationships and influences between different types of drought, the dynamic change of drought propagation and the quantitative estimation of various influencing factors on its dynamics at seasonal scale remain unsolved. Improving the understanding of the mechanisms of drought propagation can help water resource managers to design optimal water management strategies, which may be used to mitigate the impacts of droughts. However, propagation in diverse types of drought needs further and systematic research. The numerous mechanisms behind drought propagation require to be explored in depth. To fill this research gap, the study attempts to examine the propagation time from meteorological to hydrological drought in different seasons, and analyzes their dynamic changes, for evaluating the drought propagation dynamics. With the modification of precipitation deficits in drought propagation, diverse climate, different basins as well as human activities make an important contribution, leading to the diversity of drought propagation in different catchments (Van Loon 2015). Thereupon, examining the different types of drought and how drought propagates is the top priority. It can boost the acquaintance of drought, create the foundation to support the development of drought and predict the variation tendency of drought.

This study has the following three main objectives: (1) to calculate the propagation time from meteorological drought to hydrological drought at seasonal scale; (2) to examine the seasonal dynamic propagation characteristics under the backdrop of a changing environment and (3) to quantitatively explore the impacts of meteorology, underlying surface features, teleconnection factors on seasonal dynamic propagation.

2. STUDY AREA AND DATASET

2.1. Study area

The Wei River Basin (WRB) is the largest tributary of the Yellow River basin, which covers an area of 134,600 km^2. The distribution map of the WRB is shown in Figure 1. This basin is located in the continental monsoon climate zone with abundant precipitation and high temperature in summer, little precipitation and low temperature in winter. Generally speaking, precipitation has a significant seasonal variation. During monsoon (June–September), precipitation accounts for 60% of whole year's precipitation, which always appears in the form of rainstorm or continuous rain. Owing to the uneven annual distribution and large inter-annual variation of precipitation in this area, which are mainly caused by the instable intensity of the North Pacific subtropics. The annual maximum precipitation can be 2.5 times larger than the annual minimum precipitation. Since ancient times, natural disaster events have frequently occurred in this basin (Du 2008), especially for drought events, which is the most frequent and harmful disaster. Drought has become the main factor restricting the regional development.

The Wei River is the main water source of the Guanzhong Plain, which is an area where agriculture plays a crucial role in local economic development (Huang *et al.* 2017). With the rapid development, this zone has also built many industrial parks, whose functioning requires water (Huang *et al.* 2017). The runoff in the WRB has obviously reduced in recent decades (Huang *et al.* 2014a, 2014b), and it was often subjected to the effect of droughts (Huang *et al.* 2014a, 2014b). Hence, the WRB is a region with extreme shortage of water. A comprehensive drought investigation integrated with the drought propagation and its influence is of great important in mitigating the drought effects.

2.2. Data

In this paper, daily precipitation data were collected from 1960 to 2010 from 21 weather stations in the WRB, which derived from the National Climate Center of the China Meteorological Administration. The runoff data were obtained from the Yellow River conservancy commission, including daily runoff sequences from 1962 to 2010 from several hydrological stations in Linjiacun, Zhangjiashan, Huaxian and Zhuangtou and others. The mean values of these stations are used as the calculated data of the WRB in this study. The El Niño-Southern Oscillation (ENSO) events are represented by the monthly Nino 3.4

Index and the monthly Arctic Oscillation (AO) series containing 1962–2010 events obtained from the National Oceanic and Atmospheric Administration (NOAA). Daily sunspot data from 1962 to 2010 supplied by the International Council for Science (ICSU) World Data System (WDS) and the long-term observational series were used in this study (http://sidc.oma.be/silso/dayssnplot). Additionally, potential evapotranspiration series of the meteorological stations were calculated through the Penman–Monteith equation (Allen *et al.* 1989). The soil moisture and base flow data were both simulated by the Variable Infiltration Capacity (VIC) model.

3. METHODOLOGIES

3.1. Standardized Precipitation Index

It is hard to compare changes in diverse spatial–temporal scale utilizing the precipitation data straightly due to the high fluctuation of precipitation in different times and districts. Moreover, the distribution of precipitation is a skewed distribution. On that basis, McKee *et al.* (1993) first brought up the conception of SPI to address a variety of time scales, which can monitor long-term precipitation conditions. The SPI can transform the skewness distribution to normal distribution, which is not only convenient for different data comparisons, but also can eliminate spatial and temporal distribution differences. At present, many studies have applied the SPI to characterize the meteorological arid conditions in the WRB and all have good results (Huang *et al.* 2014a, 2014b; Cai *et al.* 2018).

SPI is derived from a long-term record of precipitation, which is further transformed into standard normal distribution. In the first place, the original precipitation observations are aggregated to generate a precipitation series at a timescale of interest (typically 1, 3, 6 or 12 months). Then, the gamma probability distribution function is used to fit the average precipitation sequence. At last, the cumulative probability of the gamma distribution is converted to the standard normal distribution to calculate the SPI. The detail calculation process of SPI is introduced by Fang *et al.* (2019b).

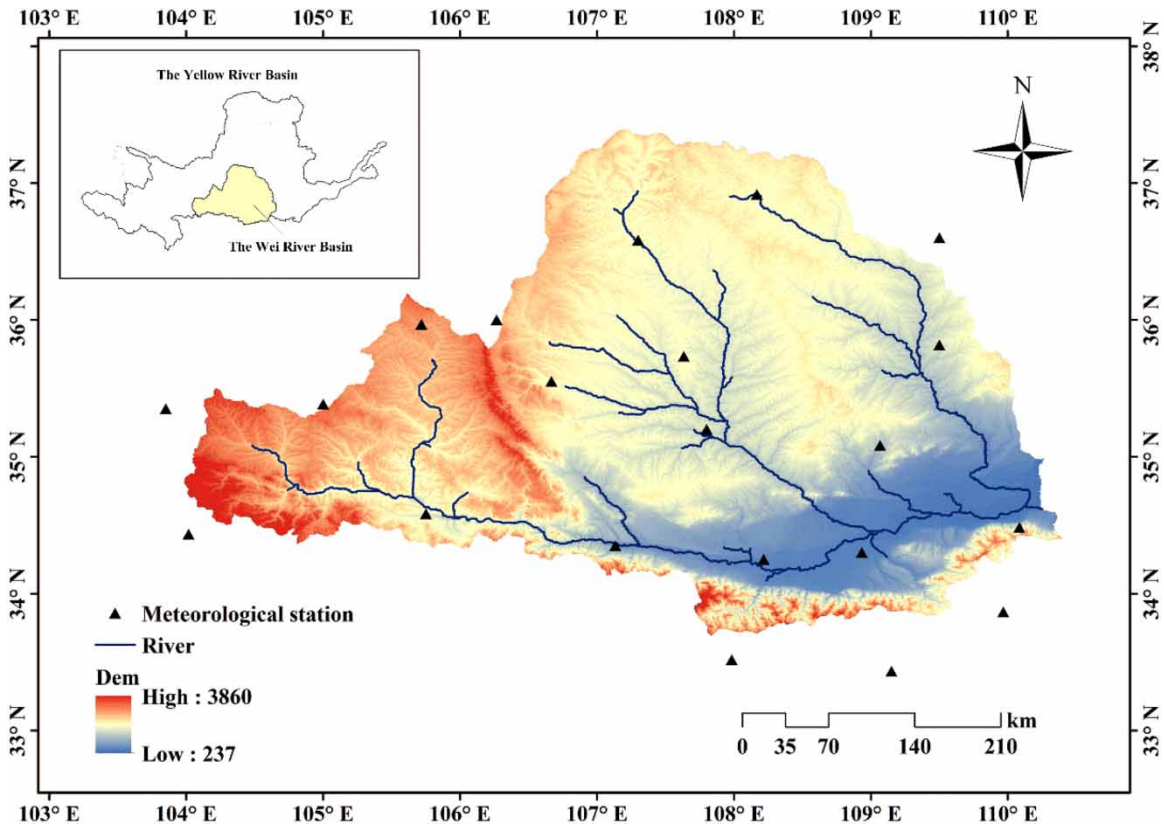

Figure 1 | Distribution map of the WRB belonging to the Yellow River Basin, China.

3.2. Standardized Runoff Index

The SRI was put forward on the strength of SPI theory used by McKee *et al.* (1993). Also, it was first proposed by Shukla & Wood (2008). Compared to the SPI, they take the same principles to build only using the different preliminary. That is to say, the calculation of SRI substitutes the runoff series for precipitation series of SPI. The calculation of SRI is to transform the distribution of accumulated runoff on a given time scale into a standard normal distribution through equal probability transformation.

3.3. Calculation of propagation time from meteorological to hydrological drought

In fact, the propagation from meteorological drought to hydrological drought is the conversion process from precipitation to runoff. Based on the multi-scale property of SPI, the scale range of SPI is changed, the scale range of SRI is fixed and then the correlation coefficient between the SPI in a variable scale and the SRI can be calculated. The SPI is chosen at the scale of 1–24 months and the SRI at 1 month in this study. Then, the correlations of SPI sequences at different time scales and SRI sequences are all calculated, respectively. Finally, the SPI scale corresponding to the maximum correlation coefficient is regarded as the propagation time from meteorological to hydrological drought (Yu *et al.* 2018; Wang *et al.* 2019).

The greatest advantage of the SPI is that it can characterize drought conditions at different scales, which would be perfectly applied on not only short-term, but also long-term, water resource monitoring. To investigate the propagation time from meteorological to hydrological drought, the relationship between the SRI and the SPI at different time scales in the WRB is explored, and related results are displayed in Figure 2. In the figure, the x coordinate signifies various time scales of SPI (1, 2, 3, …, 24), while the y coordinate displays months. Different colors imply the correlation coefficients of SPI and SRI, where red represents the high value region and blue represents the low value region of the correlation coefficient.

3.4. The cross-wavelet

The cross-wavelet is capable of presenting the correlation between two time series in both time and frequency domains, combined with the wavelet transformation and cross-spectrum analysis (Hudgins & Huang 1996). In the figure, the red represents the peak value of energy density, and the blue represents the valley value of energy density, respectively, showing the locality and dynamic characteristics of time-sharing transformation of the dominant wave group. The dark or light color represents the relative change of energy density. The fine solid black line represents the boundary of the cone line affected by the wavelet, and its interior is an effective spectral value region. The thick black line in the region represents a 95% confidence interval with a passing significance level of $A = 0.05$. The direction of the arrows in the figure reflects the phase relationship between

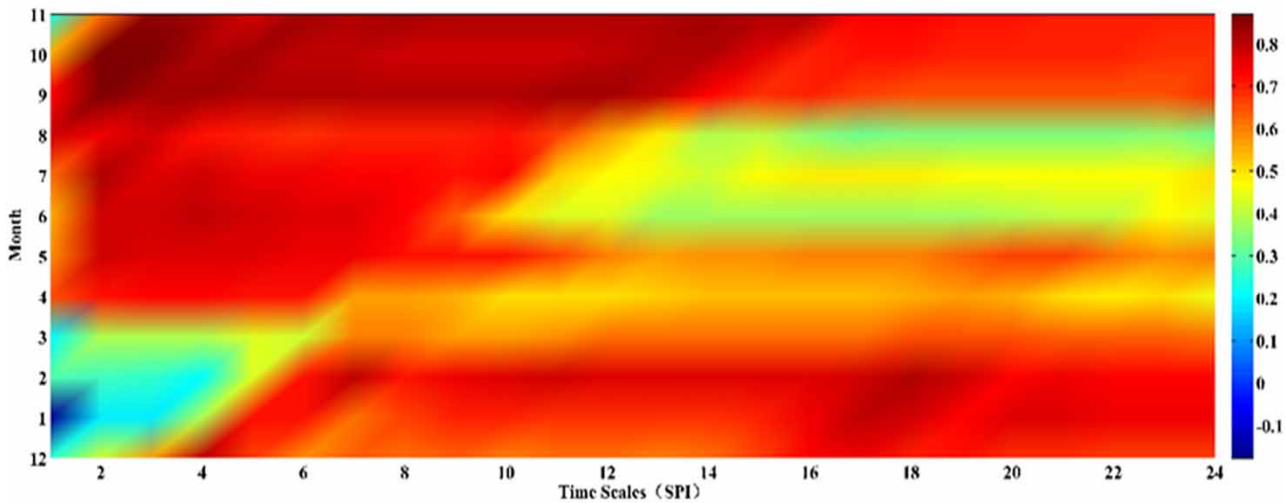

Figure 2 | Relationship between the 1-month SRI and the SPI at different time scales in the WRB. Please refer to the online version of this paper to see this figure in colour: http://dx.doi.10.2166/nh.2021.006.

the influencing factors and rainfall erosivity. The (→) from left to right indicates that the changes in the two factors are in the same phase, showing a positive correlation. The (←) from the right finger to the left represents the inverse phase, showing a negative correlation (Grinsted *et al.* 2004).

3.5. Multiple linear regression model

Multiple linear regression (MLR) is a statistical technique that attempts to model the relationship between two or more explanatory variables and a response variable by fitting a linear equation to observed data. Every value of the independent variable x is associated with a value of the dependent variable y. Formally, the model for MLR, given n observations, is

$$yi = \beta_0 + \beta_1 xi1 + \beta_2 xi2 + \cdots + \beta_p xip + c \ (i = 1, 2, \ \ldots \ , n) \tag{1}$$

MLR is used to determine a mathematical relationship among a number of random variables. In other terms, MLR examines how multiple independent variables are related to one dependent variable. Once each of the independent factors have been determined to predict the dependent variable, the information on the multiple variables can be used to create an accurate prediction on the level of effect they have on the outcome variable. The model creates a relationship in the form of a straight line (linear) that best approximates all the individual data points.

4. RESULTS AND DISCUSSION

4.1. Propagation time from meteorological to hydrological drought in different seasons

The relationship of the SPI and the SRI between 1962 and 2010 in the WRB was explored. The outcome reflects the response time of hydrological drought to meteorological drought is roughly 3 months corresponding to the coefficient of 0.870. The propagation time is short in summer and autumn, but relatively long in spring and winter. In terms of the correlation coefficient of all months, the maximum appears in October, and the autumn has the strongest correlation.

Generally, the WRB is strongly affected by monsoon, which has abundant precipitation and high temperature in summer, dry and cold climate occurs in winter. The annual average temperature is about 6–14 °C, and the annual average precipitation is 450–700 mm (Huang *et al.* 2015).

Summer (June–August) and autumn (September–November) are wet seasons. Temperature is relatively high in these two seasons, especially in summer. Its average temperature reaches 24 °C. Precipitation is always abundant (average 161.6 mm in autumn and 286.4 mm in summer in 1962–2010) with high-intensity rainstorms (Table 1). Once precipitation occurs, it is easy to generate runoff since soil moisture is high. After precipitation replenishes the interception, infiltration and sink filling, the loss is no longer significantly increased with the continuation of precipitation, and the soil is basically saturated, resulting in the generation of runoff (Apurv *et al.* 2017; Joo *et al.* 2020). The amount and intensity of the precipitation in summer and autumn are large. Therefore, the time of drought propagation is always short in the two seasons. Table 1 shows that the amount of the precipitation in summer is more than autumn, and land surface converge, therefore, tends to be faster. As a result, the propagation time in summer is shorter than that in autumn. It is indicated in Table 1 that spring (March–May) and winter (December–February) are dry seasons with little precipitation, especially in winter (120.6 mm in spring and 18.0 mm in winter in 1962–2010), and temperature is relatively low in these two seasons, especially in winter, and its average temperature is −1 to −3 °C (Jiang *et al.* 2012). Almost all of the runoff is supplied by groundwater discharge in the form of base flow in dry seasons, which is generally derived from long-term precipitation accumulation of early period (Apurv *et al.* 2017). It is found that the runoff in this region mainly depends on groundwater formed by the accumulation of precipitation in the previous 8 months in spring and 13 months in winter. The slow development of water cycle results in few runoff generation. In consequence, the process of drought propagation tends to

Table 1 | Propagation time from meteorological to hydrological drought and related meteorology information

Statistic	Spring	Summer	Autumn	Winter
P (mm)	120.6	286.4	161.6	18.0
T (month)	8	2	3	13

be slow. Moreover, the propagation time in winter is longer than that in spring mainly caused by less precipitation and cold weather. The runoff in spring comes from both groundwater and direct surface runoff, thus leading to faster propagation than winter.

4.2. Seasonal dynamic propagation characteristics from meteorological to hydrological drought

Figure 3 shows the trends of propagation time in different seasons, which is derived from a sliding window with 20-year length between 1962 and 2010. Then, the Mann–Kendall test was used to verify the significance of these trends. Specifically, Table 2 indicates that the propagation time has a significant decreasing trend in winter and a significant increasing trend in autumn at the 99% confidence level. The propagation time has no obvious tendency in spring and summer. Results indicate that the hydrologic circle rate is intensifying in winter and reducing in autumn in the Loess Plateau watershed under the warming climate. The possible causes of the propagation dynamics are systematically investigated in the next section.

4.3. Effects of diverse influencing factors on seasonal dynamic propagation

Table 2 shows the correlation between influencing factors and propagation time in different seasons. The tendency of meteorological factors and underlying surface features is shown in Table 3. It can be found that the arid index also has an insignificant decreasing trend, while precipitation has an insignificant increasing trend in summer (Table 3). It indicates that the region in summer is wetter than before, which tends to make the propagation process faster. The significant decreasing trends of base flow and soil moisture require more water to replenish them first, thus making the propagation process slower. Besides, base flow and soil moisture all have better correlation with propagation time than precipitation and arid index. As a consequence, the interaction of insignificant increasing precipitation and significant decreasing soil moisture eventually results in the insignificant increasing propagation time in summer. It indicates that underlying surface features are major influencing factors.

Results in Table 3 also indicated that the precipitation has a significant downtrend at the 95% confidence level, and the arid index has a significant uptrend at the 95% confidence level in autumn. These two factors lead to the basin becoming drier, and the significant decreasing precipitation causes the decrease of runoff, thus making the propagation process slower. In

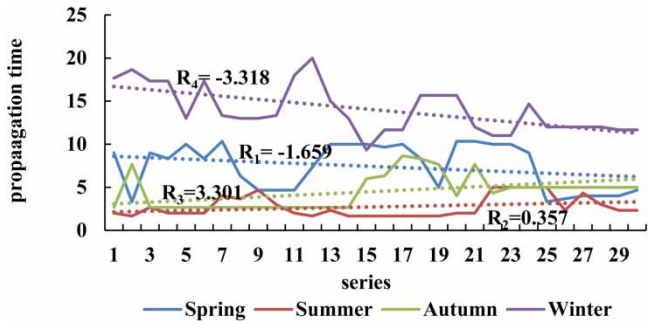

Figure 3 | Seasonal variation tendency of propagation time in the WRB.

Table 2 | Correlation between propagation time and meteorological factors, underlying surface features and teleconnection factors

	Meteorological factors			Underlying surface features		Teleconnection factors			
CC	P	ET_0	AI	SM	BF	SP	ENSO	PDO	AO
Spring	−0.598**	−0.093	0.561**	0.329*	0.261	0.474**	0.0182	−0.439**	−0.322*
Summer	−0.251	0.322*	0.296*	−0.318*	−0.315*	−0.596**	0.0177	0.238	0.227
Autumn	0.245	−0.467**	−0.368*	−0.176	−0.064	0.201	0.752**	0.560**	0.674**
Winter	0.604**	−0.567**	−0.601**	0.598**	0.617**	0.260	−0.556**	−0.515**	−0.200

CC, correlation coefficients; ET_0, potential evapotranspiration; P, precipitation; AI, aridity index; SP, sunspots; SM, soil moisture; BF, base flow.
*Significant at the 95% confidence level.
**Significant at the 99% confidence level.

Table 3 | Tendency of meteorological factors and underlying surface features

	Meteorological factors			Underlying surface features	
Influencing factors	**P**	**ET_0**	**AI**	**BF**	**SM**
Spring	−2.043*	1.715	1.871	−3.178**	−5.872**
Summer	0.422	−2.447*	−0.888	−2.328*	−3.440**
Autumn	−2.301*	0.089	2.060*	−1.635	−4.630**
Winter	1.543	−0.642	−1.612	−1.138	−4.473**

*Significant at the 95% confidence level.
**Significant at the 99% confidence level.

addition, base flow and soil moisture significantly decrease, especially for soil moisture. The replenishment of soil moisture needs more time, and the propagation time prolongs. As a result, both significant decreasing precipitation and soil moisture eventually lead to the significant increasing propagation time in autumn. This is the reason why the propagation time is more significantly increasing in autumn than that in summer.

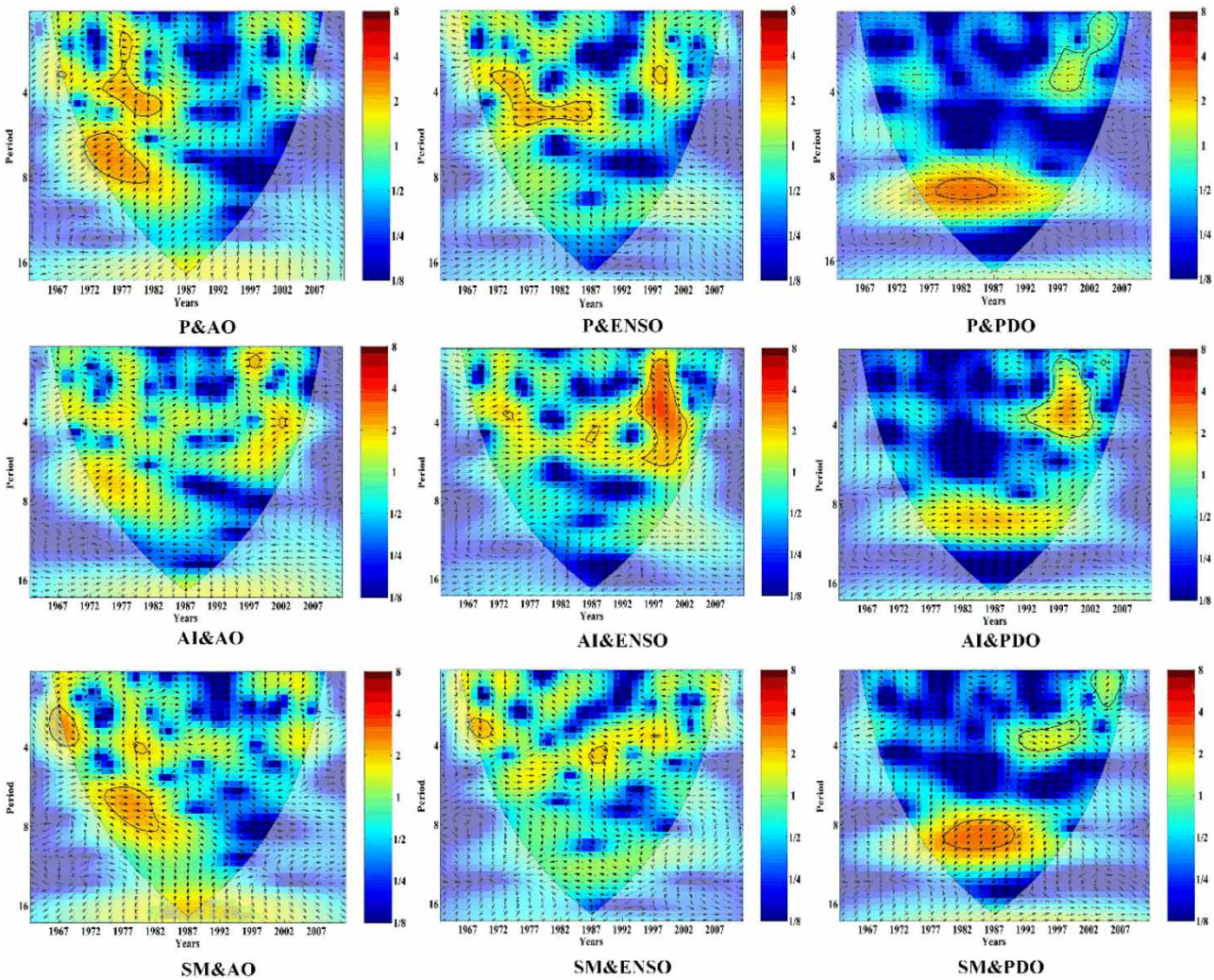

Figure 4 | Cross-wavelet of meteorological drought, underlying surface features and teleconnection factors exceeding the significance level in autumn.

Similarly, as noted in Table 3, a small amount of precipitation and high evapotranspiration cause scarce runoff generation, and the basin gets drier in winter. Streamflow in winter is reliant on groundwater supply, which is closely associated with the surface streamflow condition. Decreasing soil moisture and base flow tend to make surface streamflow exhaust earlier, thus leading to earlier replenishment of groundwater. Thus, the propagation time in winter has a significant decreasing trend. With regard to spring, its runoff is mainly impacted by precipitation and groundwater, where groundwater is the dominant factor due to the long propagation. Being similar with winter, decreasing soil moisture and base flow are expected to make surface streamflow exhaust earlier, thus resulting in earlier replenishment of groundwater. This leads to the faster propagation time. However, precipitation exhibits a significant downward trend at the 95% confidence level in spring, which causes a slower propagation time in the form of direct surface streamflow. Influenced by decreasing precipitation and earlier groundwater supply, the propagation time shows an insignificant decreasing trend.

The above results indicate that both meteorological factors and underlying surface features have a great impact of the dynamic changes of propagation time in autumn and winter. However, since the teleconnection factors can indirectly affect the propagation of drought, the study selects relatively significant influencing factors to explore the relationship between teleconnection factors and meteorological factors, as well as underlying surface features in these two seasons.

On the whole, the teleconnection factors have great influences on meteorological factors and underlying surface features. Specifically, the influence and correlation of different factors are different in autumn and winter.

The cross-wavelet analysis shown in Figure 4 indicated that the precipitation in autumn shows a significant positive correlation of about 6–8 years in 1972–1980 and a significant negative correlation of about 4–6 years in 1975–1984 with AO; the precipitation and ENSO have a significant negative correlation of about 4–6 years in 1970–1987; the precipitation and PDO have a significant negative correlation of about 9 years in 1979–1987, a significant negative correlation of about 2–4 years in 1997–2002 and a significant positive correlation about 2 years in 2002–2005. The arid index and AO have only a significant positive correlation of about 2 years in 1997–2000; the arid index and ENSO have a significant negative correlation of about 2–4 years in 1995–2000 and a significant positive correlation of about 4–6 years in 1995–2000; the arid index and PDO have a significant positive correlation of about 2–4 years in 1992–2002. The soil moisture and AO have a significant negative correlation of about 2–4 years in 1967–1970 and a significant positive correlation about 6–8 years in 1975–1982. The soil moisture and ENSO have a significant negative correlation of about 3 years in 1967–1972 and a significant negative correlation of about 4 years in 1987–1990. The soil moisture and PDO have a significant negative correlation of about 8 years in 1979–1990, a significant positive correlation of about 4 years in 1992–2002 and a significant negative

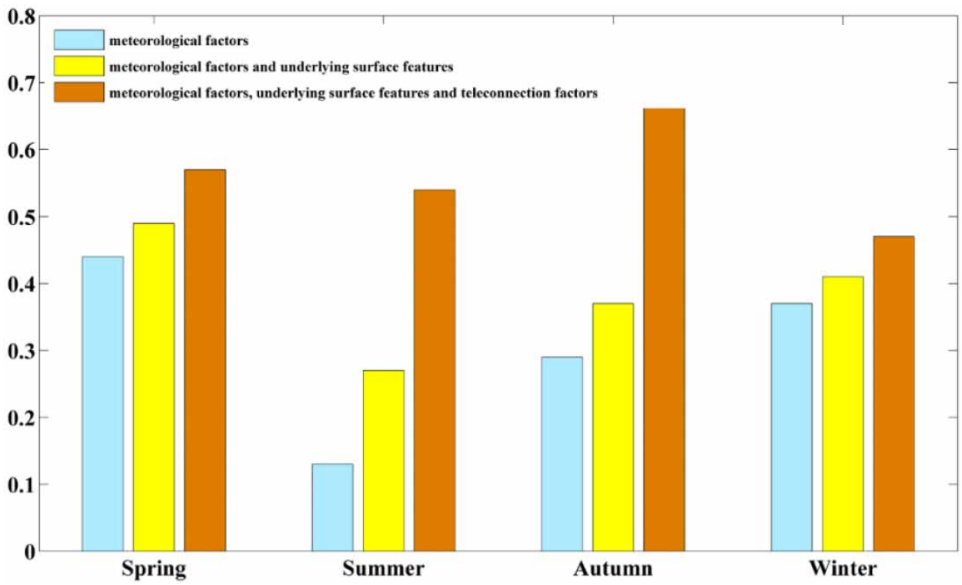

Figure 5 | Determination coefficient (R^2) and significance of the multiple linear regression model between propagation time and influencing factors. '*' represents significance at the 95% confidence level.

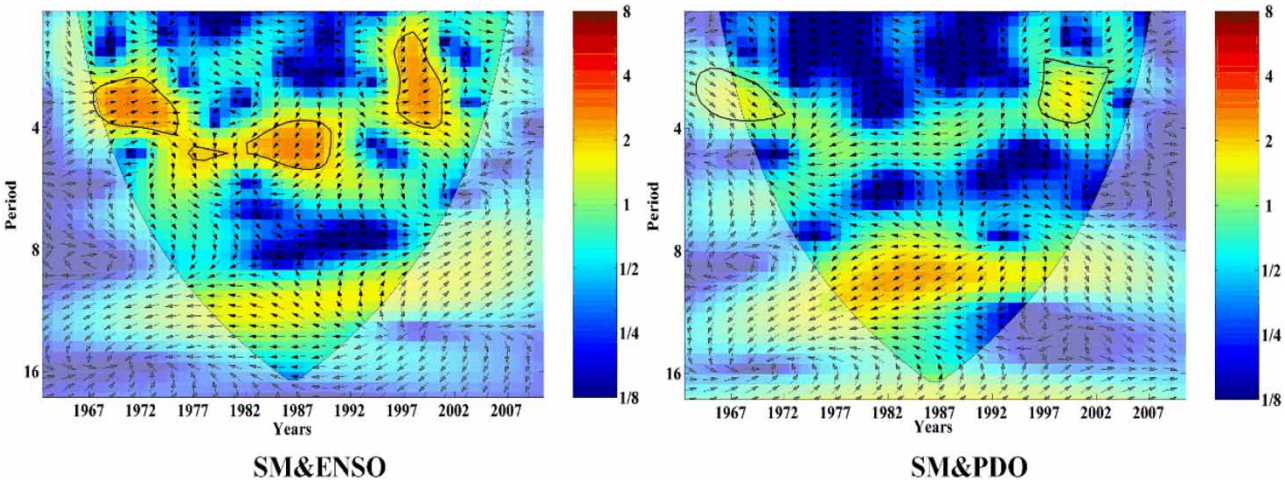

Figure 6 | Cross-wavelet of meteorological drought, underlying surface features and teleconnection factors exceeding the significance level in winter.

correlation of about 2 years in 2004–2007. In winter, the soil moisture and ENSO have a significant positive correlation of about 2–4 years in 1969–1975, a significant negative correlation of about 4–6 years in 1982–1990, a significant positive correlation of about 2–4 years in 1997–2000; the soil moisture and PDO have a significant positive correlation of about 2–4 years in 1967–1972 and 1997–2004.

It can be found from the above results that the teleconnection factors have great influences on meteorological factors and underlying surface features, and then affect the propagation time of drought.

4.4. Quantitative impacts of meteorology, underlying surface features and teleconnection factors on seasonal dynamic propagation

The above section reveals that different seasons have distinct influence factors. For better understanding the relationship between propagation and relevant factors, the MLR is built and the determination coefficient (R^2) is calculated, which are shown in Figure 5. Notably, three scenarios were designed to explore the contribution of meteorological factors, surface features and teleconnection factors. The maximum R^2 of this model fitting is 0.76, which has a certain reliability. The explanation of meteorological factors to the propagation time between meteorological and hydrological drought is 44, 12, 28 and 37% in spring, summer, autumn and winter. Whereas, when the underlying surface features are added, the explanation increased to 49, 27, 37 and 41%, respectively. And when the teleconnection factors were considered, the results have further improved and reached to 57, 54, 76 and 47%. From the above results, it can clearly be seen that the interpretation of propagation time response to underlying surface features is 5, 13, 9 and 4% in different seasons. And the interpretation of propagation time response to teleconnection factors is 8, 27, 39 and 6%, respectively. By comparison, the meteorological factors have the strongest impact on spring and winter, and the teleconnection factors have the strongest impact on summer and autumn. Therefore, the significant slowing drought of propagation patterns in autumn is closely linked with teleconnection factors.

It is obvious that considering the underlying surface features and teleconnection factors will have a better performance of drought propagation, especially in summer and autumn, which is in line with the results outlined in Figures 4 and 6 of section 'Effects of diverse influencing factors on seasonal dynamic propagation', further verifying the reliability of these findings. That is to say, taking the underlying surface features and teleconnection factors into account gives a more accurate interpretation of propagation time response.

5. CONCLUSION

In this study, the propagation dynamics from meteorological to hydrological drought and influence factors have been revealed. The following conclusions can be reached:

- The propagation time from meteorological drought to hydrological drought is generally the quickest in summer (2 months), followed by autumn (3 months), then spring (8 months) and finally winter (13 months).
- The propagation time insignificantly increases in summer and decreases in spring, while significantly increasing in autumn and decreasing in winter.
- The results indicate that AO, ENSO and PDO in autumn; ENSO and PDO in winter have great impacts.

Although the paper has determined the responding time of hydrological drought to meteorological drought in seasons and dynamic changes, and the impacts on propagation process, it also found that considering the teleconnection factors will have a better performance of drought propagation. And the study has provided the basis for drought researchers and forecasters. But the further influencing mechanism has not been revealed. How other factors impact the drought propagation needs to be studied for further investigation.

ACKNOWLEDEGMENTS

This study was jointly funded by the National Key Research and Development Program of China (grant no. 2017YFC0405900), the Strategic Priority Research Program of the Chinese Academy of Sciences (Grant No. XDA28060100), the National Natural Science Foundation of China (grant no. 51709221), the Planning Project of Science and Technology of Water Resources of Shaanxi (grant nos 2015slkj-27 and 2017slkj-19), the Open Research Fund of State Key Laboratory of Simulation and Regulation of Water Cycle in River Basin (China Institute of Water Resources and Hydropower Research, grant no. IWHR-SKL-KF201803), and the Doctorate Innovation Funding of Xi'an University of Technology (grant no. 310-252071712).

DATA AVAILABILITY STATEMENT

All relevant data are available from an online repository or repositories Meteorological data come from China Meteorological Data Network (http://data.cma.cn/). Sunspot data come from International Council for Science World Data System (http://sidc.oma.be/silso/dayssnplot). ENSO (Nino3.4) & AO (Arctic Oscillation) & PDO (Pacific Decadal Oscillation) come from National Oceanic and Atmospheric.

REFERENCES

Allen, R. G., Jensen, M. E., Wright, J. L. & Burman, R. D. 1989 Operational estimates of reference evapotranspiration. *Agronomy Journal* **81** (4), 650–662.

Apurv, T., Sivapalan, M. & Cai, X. 2017 Understanding the role of climate characteristics in drought propagation. *Water Resources Research* **53** (11), 9304–9329.

Brekke, A. 1947 *Drought, Its Causes and Effects, Ivan Ray Tannehill*. Princeton University Press, Princeton, NY. 264 pp. https://doi.org/10.2307/1232917.

Cai, S. Y., Zuo, D. P., Xu, Z. X. & Han, X. M. 2018 Spatiotemporal variability and assessment of drought in the Wei River basin of China. *Proceedings of the International Association of Hydrological Sciences (IAHS)* **379**, 73–82. https://doi.org/10.5194/piahs-379-73-2018.

Chen, H. & Sun, J. 2017 Anthropogenic warming has caused hot droughts more frequently in China. *Journal of Hydrology* **544**, 306–318. https://doi.org/10.1016/j.jhydrol.2016.11.044.

Cook, E. R., Meko, D. M., Stahle, D. W. & Cleaveland, M. K. 1999 Drought reconstruction for the continental United States. *Journal of Climate* **12**, 1145–1162. https://doi.org/10.1175/1520-0442(1999)012,1145:DRFTCU.2.0.CO;2.

Dracup, J. A., Lee, K. S. & Paulson Jr., E. G. 1980 On the definition of droughts. *Water Resources Research* **16** (2), 297–302. https://doi.org/10.1029/wr016i002p00297.

Du, J. W. 2008 *Drought Monitoring Forecasting Assessment and Hazard Management in Shaanxi Province*. China Meteorological Press, Xi'an (in Chinese).

Fang, W., Huang, S. Z., Huang, Q., Huang, G. H., Wang, H., Leng, G. Y., Wang, L. & Guo, Y. 2019a Probabilistic assessment of remote sensing-based terrestrial vegetation vulnerability to drought stress of the Loess Plateau in China. *Remote Sensing of Environment* **232**, 111290. https://doi.org/10.1016/j.rse.2019.111290.

Fang, W., Huang, S., Huang, G., Huang, Q., Wang, H., Wang, L., Zhang, Y., Li, P. & Ma, L. 2019b Copulas-based risk analysis for inter-seasonal combinations of wet and dry conditions under a changing climate. *International Journal of Climatology* **39** (4), 2005–2021. https://doi.org/10.1002/joc.5929.

Feng, P., Hu, R. & Li, J. Z. 2014 Meteorological drought grade prediction using three-dimensional log-linear models. *Journal of Hydraulic Engineering* **45** (5), 505–512.

Fye, F. K., Stahle, D. W. & Cook, E. R. 2010 Paleoclimatic analogs to twentieth-century moisture regimes across the United States. *Bulletin of the American Meteorological Society* **84** (7), 901–910. https://doi.org/10.1175/BAMS-84-7-901.

Ge, Y., Apurv, T. & Cai, X. 2016 Spatial and temporal patterns of drought in the Continental U.S. during the past century. *Geophysical Research Letters* **43** (12), 6294–6303. https://doi.org/10.1002/2016GL069660.

Grinsted, A., Moore, J. C. & Jevrejeva, S. 2004 Application of the cross wavelet transform and wavelet coherence to geophysical time series. *Nonlinear Processes in Geophysics* **11** (5/6), 561–556.

Guo, Y., Huang, S., Huang, Q., Wang, H., Fang, W., Yang, Y. & Wang, L. 2019 Assessing socioeconomic drought based on an improved Multivariate Standardized Reliability and Resilience Index. *Journal of Hydrology* **568**, 904–918. https://doi.org/10.1016/j.jhydrol.2018.11.055.

Huang, S. Z., Chang, J. X., Huang, Q. & Chen, Y. T. 2014a Spatio-temporal changes and frequency analysis of drought in the Wei River Basin, China. *Water Resource Management* **28** (10), 3095–3110. https://doi.org/10.1007/s11269-014-0657-4.

Huang, S. Z., Chang, J. X., Huang, Q. & Chen, Y. T. 2014b Monthly streamflow prediction using modified EMD-based support vector machine. *Journal of Hydrology* **511**, 764–775. https://doi.org/10.1016/j.jhydrol.2014.01.062.

Huang, S. Z., Huang, Q., Wang, Y. M. & Chen, Y. T. 2015 Evolution of drought characteristics in the Weihe River Basin based on standardized precipitation index. *Journal of Natural Disasters* **24**, 15–22.

Huang, S. Z., Li, P., Huang, Q., Leng, G. Y., Hou, B. B. & Ma, L. 2017 The propagation from meteorological to hydrological drought and its potential influence factors. *Journal of Hydrology* **547**, 184–195. https://doi.org/10.1016/j.jhydrol.2017.01.041.

Huang, S., Wang, L., Wang, H., Huang, Q., Leng, G. & Fang, W. 2019 Spatio-temporal characteristics of drought structure across China using an integrated drought index. *Agricultural Water Management* **218**, 182–192. https://doi.org/10.1016/j.agwat.2019.03.053.

Hudgins, L. & Huang, J. 1996 Bivariate wavelet analysis of Asia monsoon and ENSO. *Advances in Atmospheric Sciences* **13** (3), 299–312. https://doi.org/10.1007/bf02656848.

Jiang, C., Wang, F., Xing-Min, M. U. & Rui, L. I. 2012 Temporal and spatial characteristics of climate change and extreme dry and wet events in Wei River Basin in Last 52 years. *Journal of Irrigation and Drainage.* **31** (04), 32–36.

Joo, J., Jeong, S., Zheng, C., Park, C. E., Park, H. & Kim, H. 2020 Emergence of significant soil moisture depletion in the near future. *Environmental Research Letters* **15** (12), 124048 (9 pp).

Leng, G. Y., Tang, Q. H. & Rayburg, S. 2015 Climate change impacts on meteorological, agricultural and hydrological droughts in China. *Global and Planetary Change* **126**, 23–34. https://doi.org/10.1016/j.gloplacha.2015.01.003.

Li, J., Guo, Y., Wang, Y., Lu, S. & Chen, X. 2018 Drought propagation patterns under Naturalized condition using daily hydrometeorological data. *Advances in Meteorology* **2018** (2), 1–14. https://doi.org/10.1155/2018/2469156.

Lorenzo-Lacruz, J., Vicente-Serrano, S. M., Gonzalez-Hidalgo, J. C., Lopez-Moreno, J. I. & Cortesi, N. 2013 Hydrological drought response to meteorological drought in the Iberian Peninsula. *Climate Research* **58** (2), 117–131. https://doi.org/10.3354/cr01177.

McKee, T. B., Doesken, N. J. & Kleist, J. 1993 The Relation of Drought Frequency and Duration to Time Scales. Proceedings of the 8th Conference on Applied Climatology, Anaheim, California, 17–22 January 1993, pp. 179–184.

Mishra, A. K. & Singh, V. P. 2010 A review of drought concepts. *Journal of Hydrology* **391** (1–2), 202–216. https://doi.org/10.1016/j.jhydrol.2010.07.012.

Mohammad, R. K., Majid, V. & Amin, A. 2014 Drought monitoring using a Soil Wetness Deficit Index (SWDI) derived from MODIS satellite data. *Agriculture Water Management* **132** (31), 37–45. https://doi.org/10.1016/10.1016/j.agwat.2013.10.004.

Shukla, S. & Wood, A. W. 2008 Use of a standardized runoff index for characterizing hydrologic drought. *Geophysical Research Letters* **35** (2), 226–236. https://doi.org/10.1029/2007gl032487.

Tallaksen, L. M. & Van Lanen, H. A. J. 2004 Hydrological drought: process and estimation methods for streamflow and groundwater. In: *Developments in Water Science*. 48. Elsevier Science, Amsterdam.

Tallaksen, L. M., Hisdal, H. & Van Lanen, H. A. 2009 Space–time modelling of catchment scale drought characteristics. *Journal of Hydrology* **375** (3), 363–372. https://doi.org/10.1016/j.jhydrol.2009.06.032.

Van Loon, A. F. 2015 Hydrological drought explained. *Wiley Interdisciplinary Reviews: Water* **2** (4), 359–392. https://doi.org/10.1002/wat2.1085.

Van Loon, A. F. & van Lanen, H. A. J. 2012 A process-based typology of hydrological drought. *Hydrology and Earth System Sciences* **16** (7), 1915–1946. https://doi.org/10.5194/hess-16-1915-2012.

Wang, D. B., Mohamad, H., Cai, X. & Valocchi, A. J. 2011 Climate change impact on meteorological, agricultural, and hydrological drought in central Illinois. *Water Resources Research* **47**, 1–13, W09527.

Wang, Y., Li, J., Zhang, T. & Wang, B. 2019 Changes in drought propagation under the regulation of reservoirs and water diversion. *Theoretical and Applied Climatology*. https://doi.org/10.1007/s00704-019-02839-3.

Wilhite, D. A. & Glantz, M. H. 1985 Understanding the drought phenomenon: the rule of definition. *Water International* **10** (3), 111–120. https://doi.org/10.1080/02508068508686328.

World Meteorological Organization (WMO). 1997 *Climate, Drought and Desertification*. WMO No. 869, Geneva, 12 p.

Xu, K., Yang, D., Xu, X. & Lei, H. 2015 Copula based drought frequency analysis considering the spatio-temporal variability in Southwest China. *Journal of Hydrology* **527**, 630–640. https://doi.org/10.1016/j.jhydrol.2015.05.030.

Yu, M., Li, Q., Hayes, M. J., Svoboda, M. D. & Heim, R. R. 2014 Are droughts becoming more frequent or severe in china based on the standardized precipitation evapotranspiration index: 1951–2010. *International Journal of Climatology* **34** (3), 545–558.

Yu, M., Cho, Y., Kim, T. W. & Chae, H. S. 2018 Analysis of drought propagation using hydrometeorological data: from meteorological drought to agricultural drought. *Journal of Korea Water Resources Association* **51** (3), 195–205. https://doi.org/10.3741/JKWRA.2018.51.3.195.

Zhang, B. Q., Wu, P. T., Zhao, X. N., Wang, Y. B., Wang, J. W. & Shi, Y. G. 2012 Drought variation trends in different subregions of the Chinese Loess Plateau over the past four decades. *Agricultural Water Management* **115**, 167–177. https://doi.org/10.1016/j.agwat.2012.09.004.

First received 7 January 2021; accepted in revised form 24 November 2021. Available online 10 December 2021